Biogeochemical cycles as information-thermodynamic computational systems

By Jed Anderson and Jim Blackburn (Contributor) with Grok-4.1 Deep Research, Gemini 3.0 Pro Deep Research, Chat GPT 5.1, and Claude 4.5 Deep Research (11/23/2025)

Introduction

The water and carbon cycles function as planetary-scale computational systems that process energy and information according to fundamental thermodynamic principles, with quantifiable entropy flows bridging quantum mechanics to ecosystem organization. Recent advances reveal that **living systems augment entropy production by factors of 1,000-10,000 over abiotic Earth**, while biological information processing operates within **26-fold of fundamental Landauer limits** at **3.17×10^{-19} J per amino acid**—approximately one million times more efficiently than current supercomputers. These cycles exhibit universal scaling laws spanning 27 orders of magnitude and demonstrate that Shannon information entropy and Boltzmann thermodynamic entropy represent identical concepts differing only by Boltzmann's constant, connected through **Landauer's principle at 2.9×10^{-21} J per bit** at room temperature.

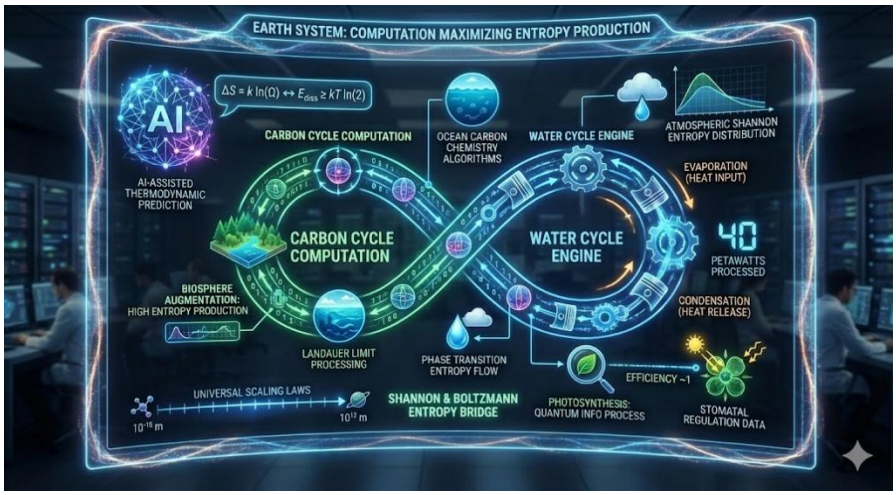

Understanding biogeochemical cycles through information-theoretic lenses enables transformative advances in environmental AI. Knowledge-guided machine learning frameworks now predict carbon fluxes with over one million times the computational speed of process-based models while revealing 86% more spatial detail, achieving this through integration of thermodynamic constraints directly into neural network loss functions. Maximum entropy production principles, while controversial, successfully predict planetary temperature distributions and provide organizing frameworks for ecosystem dynamics. The convergence of information theory, statistical mechanics, and biogeochemistry reveals that Earth's living systems operate as sophisticated computation engines that maximize entropy production over temporal scales through information storage in genetic code, organizing resource distribution through fractal networks following precise power laws, and maintaining organization far from equilibrium through continuous negentropy import from solar radiation.

Water cycle energetics: phase transitions as entropy generators

The global water cycle represents a massive thermodynamic engine processing approximately **40 petawatts** (4.0×10^{16} W) through evaporation and condensation, moving **505,000 km³ of water annually** through phase transitions that generate precisely calculable entropy changes. Each phase transition operates according to fundamental thermodynamic relationships connecting energy, entropy, and molecular organization at quantum and statistical mechanical scales.

Evaporation from Earth's surface requires **2.5×10^{6} J/kg** of latent heat energy, drawn primarily from absorbed solar radiation at **86.4 W/m²** globally averaged. This energy breaks hydrogen bonds between water molecules, increasing molecular disorder quantified by an entropy change of **6,050 J/(kg·K)** when water vaporizes at 100°C. The reverse process of condensation releases this stored latent heat to the atmosphere, driving convection and atmospheric circulation while returning entropy to the environment. Ocean evaporation dominates at **470,000 km³/yr** (86% of total), with land contributing **74,000 km³/yr** through evapotranspiration that couples tightly to photosynthesis through stomatal regulation.

Freezing and melting transitions involve smaller but significant entropy changes. Ice melting at 0°C requires **3.34×10^{5} J/kg** and increases entropy by **1,223 J/(kg·K)**, representing the entropy gain as crystalline ice structure dissolves into liquid disorder. The ratio of vaporization to fusion entropy changes (approximately 5:1) reflects the vastly greater molecular freedom in gaseous versus liquid states. Using the Boltzmann entropy formula **$S = k_B \ln(\Omega)$** where $k_B = 1.38\times10^{-23}$ J/K, these macroscopic entropy changes correspond to astronomical increases in accessible microstates—the number of molecular configurations available to the system.

The planetary energy budget reveals how phase transitions distribute solar input. Of the **1,360 W/m²** solar constant at the top of atmosphere, Earth's surface absorbs **240 W/m²** after accounting for reflection and atmospheric absorption. Surface energy partitions into latent heat flux (25% or 86.4 W/m²), sensible heat (5% or 18.4 W/m²), and net infrared radiation (17% or ~58 W/m² upward). This distribution determines climate patterns, with latent heat transport representing the primary mechanism for moving energy from tropics to poles and from surface to upper atmosphere. The 505,000 km³ annual global evaporation cycle stores **1.26×10^{24} J/year** as latent heat, creating an atmospheric energy reservoir that releases through precipitation and condensation.

Recent satellite measurements from CERES show Earth's energy imbalance has grown from **+0.42±0.48 W/m²** in 2005 to **+1.12±0.48 W/m²** in 2019, indicating accumulating heat primarily in oceans and demonstrating anthropogenic disruption of the water cycle's entropy generation patterns. Temperature dependencies complicate these calculations—latent heat of vaporization decreases from 2.5×10^{6} J/kg at 25°C to 2.26×10^{6} J/kg at 100°C, following the approximate relationship $L_v(T) = L_v(T_0) \times \exp[\Delta H_{vap}/R \times (1/T - 1/T_0)]$. These precise thermodynamic values enable quantitative analysis of how atmospheric water vapor distribution generates and dissipates entropy while driving weather systems and long-term climate patterns.

Photosynthesis thermodynamics: quantum efficiency to ecosystem carbon fixation

The photosynthetic conversion of solar electromagnetic radiation into chemical bond energy represents one of nature's most sophisticated information-thermodynamic processes, operating with **near-unity quantum efficiency** (95% for primary reactions) while converting the overall reaction **$6CO_2 + 6H_2O \rightarrow C_6H_{12}O_6 + 6O_2$** that requires a standard Gibbs free energy input of **+2,879 kJ per mole of glucose** at pH 7 and 25°C. This strongly endergonic reaction (positive ΔG) proceeds only through coupling to exergonic light absorption, demonstrating how living systems maintain local low-entropy organization by importing negentropy from the low-entropy photon flux emanating from the sun's hot surface.

Photosynthetic light harvesting exploits quantum mechanical principles through specialized chlorophyll molecules absorbing primarily at **440 nm (blue)** and **680 nm (red)** wavelengths. Each 680 nm photon carries **2.92×10^{-19} J** or 1.82 eV of energy. The photosynthetic apparatus requires a minimum of 8 photons to reduce one CO_2 molecule (48-60 photons per glucose under real conditions), providing total energy of **1,407 kJ/mol** at 680 nm wavelength. Comparing this energy input to the 2,879 kJ/mol Gibbs free energy stored in glucose yields a theoretical maximum efficiency of approximately **30%**, though overall photosynthetic efficiency from solar energy to biomass reaches only **3.9-4.5%** when including all losses from reflection, wrong wavelengths, respiration, and metabolic overhead.

The enthalpy change for photosynthesis is **+2,803 kJ/mol glucose**, slightly less than the Gibbs free energy due to entropy changes. The difference $\Delta G - \Delta H = T\Delta S$ reveals that photosynthesis results in a small entropy increase ($\Delta S \approx +255$ J/(mol·K)) from converting 12 molecules of reactants to 7 molecules of products, though this calculation includes only the chemical system and not the much larger entropy increase in the sun and Earth environment. Recent debates in quantum biology question whether quantum coherence observed in photosynthetic reaction centers functionally enhances efficiency. Two-dimensional electronic spectroscopy detected quantum beating signals lasting ~600 femtoseconds at 77K in the Fenna-Matthews-Olson complex, initially interpreted as long-lived coherence enabling wavelike energy transfer across multiple pathways. However, subsequent research demonstrated that at physiological temperatures (300K), electronic coherence decays in under 60 femtoseconds—likely too brief for functional significance. Current consensus suggests classical incoherent hopping suffices to explain photosynthetic efficiency, with observed oscillations primarily representing vibrational rather than electronic coherence.

Globally, photosynthesis fixes approximately **120 Gt C/year** as gross primary production, with respiration returning about **60 Gt C** to the atmosphere, leaving **60 Gt C/year** net primary productivity. This represents an annual energy capture of roughly **2×10^{21} J**, storing solar energy as reduced carbon compounds with high chemical potential. The photosynthesis-transpiration coupling links carbon and water cycles through stomatal conductance, described mathematically by the Ball-Berry model: **$g_s = m \times (A_n \times h_s/c_s) + b$** where g_s is stomatal conductance, A_n is net photosynthesis rate, h_s is relative humidity, c_s is CO_2 concentration, and m is a species-specific slope parameter ranging from 5-15. Water use efficiency (WUE = GPP/ET)

typically ranges from **1.5-3.0 g C per kg H_2O** globally, representing the carbon gain per unit water transpired. This coupling demonstrates how thermodynamic optimization at the leaf level—maximizing carbon gain while minimizing water loss—scales to ecosystem and planetary carbon-water cycle interactions.

Carbon respiration and decomposition: entropy production quantified

The reverse reaction of photosynthesis—cellular respiration oxidizing glucose to CO_2 and water—releases the stored chemical energy while generating substantial entropy. The combustion of glucose is strongly exergonic with **$\Delta H° = -2{,}803$ kJ/mol** and **$\Delta G°' = -2{,}879$ kJ/mol**, making this spontaneous in the thermodynamic sense (though kinetically controlled by enzymatic activation). Using $\Delta G = \Delta H - T\Delta S$, the entropy change for complete glucose oxidation at 298K is **$\Delta S = +260$ J/(mol·K)**, representing increased molecular disorder as one glucose molecule and six O_2 molecules (7 total) transform into 12 gaseous molecules (6 CO_2 + 6 H_2O vapor) with greater translational, rotational, and vibrational freedom.

Living organisms capture this released free energy through ATP synthesis with remarkable thermodynamic efficiency. Modern estimates indicate **30-32 ATP molecules** produced per glucose (revised downward from older estimates of 38 ATP). With ATP hydrolysis releasing **30.5 kJ/mol** under standard conditions (50-54 kJ/mol under cellular conditions with high ATP:ADP ratios), total energy stored amounts to approximately 915-1,098 kJ per glucose, yielding cellular efficiency of **38-50%**. This efficiency rivals or exceeds typical heat engines and represents operation close to thermodynamic optimality given constraints of operating at moderate temperatures, aqueous environment, and requirement for metabolic intermediate generation. The remaining 50-62% of glucose combustion energy dissipates as heat, representing obligatory entropy production from irreversible chemical reactions and proton gradient dissipation across membranes.

Detailed analysis reveals mitochondrial complexes operate at **80-90% thermodynamic efficiency** during active state 3 respiration with very high coupling (>95%) between electron transport and ATP synthesis. This approaches theoretical limits constrained by the second law and suggests billions of years of natural selection optimized these molecular machines. The energy cost per bit of biological information processing provides another perspective—ribosomal protein synthesis requires approximately **4 ATP equivalents per amino acid** added (2 for aminoacyl-tRNA synthesis, 2 for peptide bond formation), corresponding to **3.17×10^{-19} J per amino acid operation**. For a 20-letter amino acid alphabet, this represents operation at roughly **26 times above the Landauer bound** (the thermodynamic minimum $k_B T \ln(2) \approx 2.9\times10^{-21}$ J per bit at 300K). Remarkably, this makes biological information processing approximately **one million times more energy efficient** than current supercomputers operating at ~5×10^{-13} J per bit operation.

Global respiration and decomposition generate entropy at massive scales. Terrestrial net primary production of ~60 Gt C/year mostly returns to the atmosphere through respiration over timescales from hours (leaf respiration) to decades (wood decomposition). Estimating

conservatively that 55 Gt C/year respires, this releases approximately **2.1×10^{20} J/year** as heat to the environment—small compared to solar input but representing the metabolic power of the biosphere. This heat release, combined with inevitable entropy increase from irreversible reactions, means living systems dramatically amplify Earth's entropy production rate compared to an abiotic planet. Estimates suggest biotic Earth generates entropy at rates **1,000-10,000 times higher** than purely geochemical processes would achieve, supporting the maximum entropy production hypothesis that life exists because it accelerates the dissipation of thermodynamic gradients.

Ocean carbon chemistry: equilibria and buffering capacity

Ocean absorption of atmospheric CO_2 follows Henry's law with a solubility constant **$K_H = 3.3\times10^{-4}$ mol/(m³·Pa)** or **0.033 M/bar** at 25°C in seawater. Temperature strongly affects solubility through $K_H(T) = K_H(T_0) \times \exp[2400\ K \times (1/T - 1/T_0)]$, with the enthalpy of dissolution $\Delta H_{soln} \approx -24$ kJ/mol indicating exothermic absorption—warmer water holds less dissolved CO_2, creating a positive feedback where warming oceans release CO_2, further warming climate. The ocean currently absorbs **2.5±0.6 Gt C/year** (2010-2019 average), representing approximately 23% of anthropogenic emissions, though this sink shows signs of saturation and regional variability.

Once dissolved, CO_2 undergoes a complex carbonate equilibrium system that provides ocean pH buffering. Dissolved CO_2 (more precisely $CO_2 \cdot H_2O$) dissociates through two equilibrium constants at standard seawater conditions (35 salinity, 25°C): **$pK_1 = 6.0$-6.35** for the first dissociation $CO_2 + H_2O \rightleftharpoons H^+ + HCO_3^-$ ($K_1 \approx 1.0\times10^{-6}$ mol/kg) and **$pK_2 = 9.1$-10.3** for the second dissociation $HCO_3^- \rightleftharpoons H^+ + CO_3^{2-}$ ($K_2 \approx 8\times10^{-10}$ mol/kg). These equilibria, along with boric acid dissociation ($pK_B \approx 8.6$) and water dissociation ($pK_w \approx 13.8$-14.0 in seawater), determine ocean pH and carbonate chemistry speciation. Both equilibrium constants show temperature dependence with K_1 increasing approximately 4% per °C, creating complex interactions between ocean temperature, CO_2 solubility, and carbonate chemistry.

At typical surface seawater pH of 8.1, dissolved inorganic carbon (DIC) totaling **2,000-2,050 µmol/kg** distributes as approximately **90% bicarbonate ion (HCO_3^-)**, **9-10% carbonate ion (CO_3^{2-})**, and **less than 1% dissolved CO_2**. Total alkalinity of **2,300-2,350 µmol/kg** exceeds DIC, providing buffering capacity. The Revelle factor (buffer factor) quantifies the ocean's diminishing capacity to absorb additional CO_2—currently around 10, meaning a 10% increase in atmospheric CO_2 produces only a 1% increase in oceanic DIC, with the factor increasing (worsening buffering) as more CO_2 dissolves. This nonlinearity creates an information-theoretic bottleneck where the ocean's capacity to encode additional atmospheric CO_2 information decreases as the system saturates.

Calcium carbonate saturation states determine whether shells and coral skeletons precipitate or dissolve. Solubility products at 25°C and salinity 35 give **$K_{sp(calcite)} = 4.5\times10^{-7}$ mol²/kg²** and **$K_{sp(aragonite)} = 6.7\times10^{-7}$ mol²/kg²**, with aragonite roughly 1.5 times more soluble. The saturation state $\Omega = [Ca^{2+}][CO_3^{2-}]/K_{sp}$ typically ranges from **4-6 for calcite** and **3-4 for aragonite** in surface waters, indicating supersaturation that allows biological calcification. Ocean acidification from CO_2 absorption decreases pH (ocean pH has declined by **0.1 units** since

preindustrial times, representing a 30% increase in H^+ concentration), which shifts carbonate equilibria toward HCO_3^- and dissolved CO_2, reducing CO_3^{2-} concentration and thus saturation state. This threatens calcifying organisms and represents a quantifiable thermodynamic stress on marine ecosystems, with some models predicting aragonite undersaturation in polar surface waters within decades under high-emission scenarios.

Shannon entropy in atmospheric water distributions and weather prediction limits

Shannon entropy **$H(X) = -\Sigma\, p(i) \log_2(p(i))$** measures uncertainty and information content in probability distributions, providing rigorous quantification of predictability in atmospheric systems. Applied to precipitation patterns across Poland from 1901-2010 using bivariate Clayton copula functions for joint temperature-precipitation distributions, Shannon entropy values ranged from **3.753 to 4.919 bits** depending on season and region. Summer months showed highest entropy values (July: **4.769-4.780 bits**), indicating maximum unpredictability and complexity in warm-season precipitation patterns, while spring months exhibited lowest entropy (April-May: **3.753-3.786 bits**), reflecting more deterministic climatic regimes. Temporal trends reveal entropy increases of **+0.221 bits in January** and **+0.203 bits in July** over 40 years, quantifying the increasing unpredictability and variability associated with climate change as the system explores a larger region of its phase space.

Global Network of Isotopes in Precipitation (GNIP) studies applying Shannon entropy to isotopic compositions (δD and $\delta^{18}O$) demonstrate that entropy distributions reveal oceanic sources of water vapor and primary moisture transport pathways, with distinct spatial patterns between summer and winter seasons. This information-theoretic approach quantifies uncertainty in atmospheric water cycling more rigorously than traditional variance-based statistics. Tropospheric entropy generation rates prove proportional to the square of Earth's average surface temperature, connecting thermodynamic and information entropies through the fundamental relationship established by E.T. Jaynes' seminal 1957 papers in Physical Review proving that Shannon and Boltzmann/Gibbs entropy represent mathematically identical concepts differing only by Boltzmann's constant as a conversion factor.

Weather prediction faces fundamental limits from deterministic chaos discovered by Edward Lorenz in 1963 through simplified atmospheric convection equations showing sensitive dependence on initial conditions. The Lorenz attractor equations $dx/dt = \sigma(y - x)$, $dy/dt = x(\rho - z) - y$, $dz/dt = xy - \beta z$ with standard parameters $\sigma = 10$, $\rho = 28$, $\beta = 8/3$ exhibit a maximum Lyapunov exponent **$\lambda \approx 0.9$**, meaning infinitesimally close initial conditions separate exponentially with errors doubling approximately every **2-3 days**. This establishes a fundamental predictability horizon of roughly **10-15 days** for detailed weather prediction, confirmed by operational ensemble forecasting systems. Information loss occurs at a rate characterized by the Kolmogorov-Sinai entropy of approximately **0.9 bits per time unit** for the Lorenz system, quantifying how information about initial conditions erodes as trajectories explore the strange attractor's fractal structure.

The distinction between weather (chaotic individual trajectories) and climate (statistical properties of attractors) becomes critical here. While specific rainfall patterns remain unpredictable beyond two weeks, long-term statistics like seasonal average precipitation can show predictability through forced responses to boundary conditions (sea surface temperatures, greenhouse gas concentrations) that shift attractor structure. Modern ensemble prediction systems like ECMWF's 51-member ensemble operationalize chaos theory insights, with ensemble spread quantifying forecast uncertainty through information entropy of the ensemble distribution. As lead time increases, forecast entropy asymptotically approaches climatological entropy, representing complete loss of information about initial conditions. Research demonstrates predictability varies spatially and temporally, with some atmospheric states remaining predictable longer than others—a phenomenon quantifiable through local Lyapunov exponents and finite-time predictability metrics that provide information-theoretic characterization of forecast skill.

Information in DNA, cells, and ecosystems: quantifying biological complexity

The human genome's approximately 3 billion base pairs encode a maximum theoretical capacity of **6 billion bits** (2 bits per base pair with 4 possible nucleotides), equivalent to 750 megabytes. However, actual information content proves substantially lower when accounting for redundancy, non-coding regions, and evolutionary conservation. Shannon entropy analysis of codon sequences yields **5.6 bits per triplet for coding regions** and **5.82 bits for non-coding regions** against a maximum entropy of 6 bits per triplet, indicating actual information content of approximately **0.4 bits per triplet in coding regions** and **0.18 bits per triplet in non-coding DNA**. For the billion triplets in the human genome, this suggests **40-180 megabytes of actual functional information**, with compression analysis supporting this range.

Alternative calculations using evolutionary information provide another estimate. Assuming Kimura's rate of **0.29 bits added per generation** and approximately 10^8 generations since the Cambrian explosion 500 million years ago yields **10^8 bits or 12.5 megabytes**—comparable to the Shannon entropy estimates and suggesting substantial DNA serves regulatory, structural, or redundant functions rather than primary information encoding. The genetic code itself demonstrates remarkable efficiency and error-correction properties through redundancy—64 codons encoding 20 amino acids plus start/stop signals means many mutations change nucleotides without altering amino acids (synonymous mutations), providing information-theoretic buffering against transcription and replication errors.

Cellular information extends beyond genomic DNA to include epigenetic modifications, chromatin structure, metabolite concentrations, and protein interaction networks. Methylation patterns alone add at least **22,500 bits** of regulatory information to human cells, with total human genetic information including epigenetic markers estimated at **857 megabytes**. Translation efficiency approaches thermodynamic limits remarkably closely—as noted, the **4 ATP per amino acid** energy cost places biological information processing at **26× the Landauer bound** of $k_B T \ln(2)$ per bit (calculated at 3×10^{-21} J at 300K). Comparatively, synapses operate 10^5 to 10^8 times above Landauer limits, while current supercomputers function approximately **10^6 times**

less efficiently than biological translation, dissipating ~5×10^{-13} J per bit operation versus biology's 3×10^{-19} J per amino acid.

Ecosystem diversity represents another information layer. Global biodiversity estimated at 13-14 million species (with only ~1.5 million currently described) embodies vast information about successful evolutionary strategies, ecological niches, and biochemical innovations. Shannon diversity indices $H' = -\Sigma(p_i \ln p_i)$ applied to species abundance distributions quantify ecosystem complexity, with tropical rainforests exhibiting highest information content through enormous species richness and genetic diversity within species. Forest ecosystems contain approximately 80% of terrestrial biodiversity, concentrating biological information in regions with high energy throughput and nutrient cycling rates. The relationship between biodiversity and entropy production remains an active research area, with evidence that diverse ecosystems generate higher entropy through more complete utilization of available energy gradients, though complexity doesn't necessarily correlate monotonically with entropy production rates in food web models.

Jaynes' unification: maximum entropy principle connecting Shannon and Boltzmann

E.T. Jaynes' landmark 1957 papers "Information Theory and Statistical Mechanics" published in Physical Review established the profound connection that Shannon information entropy and Boltzmann/Gibbs thermodynamic entropy represent the same mathematical concept, differing only by Boltzmann's constant as a dimensional conversion factor. The Shannon entropy $\mathbf{H = -\Sigma p_i \log_2(p_i)}$ measures information in bits for discrete probability distributions, while Gibbs entropy $\mathbf{S = -k_B \Sigma p_i \ln(p_i)}$ measures thermodynamic entropy in J/K—identical functional forms. Boltzmann's famous formula $\mathbf{S = k_B \ln(\Omega)}$ emerges as the special case when all Ω microstates are equally probable, since if $p_i = 1/\Omega$ for all states, then $S = -k_B \Sigma(1/\Omega)\ln(1/\Omega) = k_B \ln(\Omega)$.

Jaynes proved that statistical mechanics emerges naturally from information theory through the maximum entropy principle: given testable information in the form of constraints (like average energy), the probability distribution that best represents our state of knowledge is the one with maximum entropy subject to those constraints. This distribution is "maximally noncommittal" regarding missing information, making minimum assumptions beyond stated constraints. Remarkably, this principle derives all fundamental distributions of statistical mechanics—Maxwell-Boltzmann, Bose-Einstein, and Fermi-Dirac—by maximizing entropy with appropriate constraints (energy conservation, particle indistinguishability, Pauli exclusion). The canonical ensemble partition function Z and Boltzmann factor $\exp(-E/k_B T)$ emerge as immediate consequences of entropy maximization with average energy constraint.

Landauer's principle provides the quantitative bridge connecting information erasure to thermodynamic cost: erasing one bit of information must dissipate at least **$k_B T \ln(2)$ joules of energy**, approximately **2.9×10^{-21} J at 300K** (room temperature). This principle, experimentally verified in multiple systems including colloidal particles, trapped ions, and nanomagnetic systems with measurements within 0.6% of theoretical predictions, establishes that information

is physical—it has mass-energy equivalence and cannot be manipulated without thermodynamic consequences. The resolution of Maxwell's demon paradox hinges on this principle: while the demon can reversibly measure molecular velocities, it must eventually erase its memory to continue operating, with this erasure dissipating entropy that compensates for the apparent second law violation.

The connection works bidirectionally. Thermodynamic entropy measures our missing information about microscopic states given macroscopic observables—for a gas with specified pressure, volume, and temperature, entropy quantifies uncertainty about which specific molecular configuration (microstate) the system occupies among the vast number consistent with those macroscopic constraints. Shannon entropy quantifies uncertainty in any probability distribution. Setting $k_B = 1$ provides direct conversion between information measured in bits and thermodynamic entropy measured in energy units. Some researchers attribute to John von Neumann the suggestion that Shannon call his measure "entropy" because "no one knows what entropy really is, so in a debate you will always have the advantage"—though apocryphal, this captures the deep equivalence these pioneers recognized. Modern information thermodynamics treats information and thermodynamic entropy as manifestations of the same fundamental quantity representing missing information about microscopic reality.

Maximum entropy production: organizing principle for living systems

The maximum entropy production (MEP) principle proposes that non-equilibrium thermodynamic systems far from equilibrium will adapt to steady states at which they dissipate energy and produce entropy at the maximum possible rate given constraints. Pioneered by Garth Paltridge in 1975 for climate modeling and developed theoretically by Roderick Dewar and Axel Kleidon, MEP has generated substantial empirical support alongside ongoing controversy about its status as fundamental principle versus statistical inference tool. Paltridge's original work demonstrated that assuming MEP in simple energy balance models successfully predicts meridional heat flux, latitudinal temperature distributions, and fractional cloud cover on Earth, with subsequent applications to Mars and Titan showing similar success.

Dewar's information-theoretic justification connects MEP to Jaynes' maximum entropy framework through non-equilibrium statistical mechanics. MEP states represent by far the most probable macroscopic configurations—realizable microscopically in overwhelmingly greater numbers of ways than other non-equilibrium steady states. This interpretation treats MEP as a statistical principle about which states systems will likely occupy rather than a dynamical law about how systems evolve. Connections to fluctuation theorems of non-equilibrium statistical mechanics provide additional theoretical grounding, though debates continue about whether MEP applies universally or only to specific system classes. Critical issues include which entropy production to maximize (material, radiative, kinetic energy dissipation may differ), over what temporal and spatial scales averaging occurs, and what constraints apply.

Applications to ecosystems reveal both successes and limitations. Quantitative testing using food web models published in Philosophical Transactions of the Royal Society B (2010 theme issue)

examined three hypotheses: (1) The fingerprint hypothesis that living communities augment entropy production over abiotic systems—**conclusively confirmed** across all models tested with living systems producing 1,000-10,000× more entropy; (2) The state selection hypothesis that among multiple possible steady states, the stable state shows highest entropy production—**partially confirmed** but breaks down with bistability; (3) The gradient response principle that increasing thermodynamic gradients produces higher entropy production in stable states—**rejected** in complex food webs with omnivory where more complex ecosystems don't necessarily show higher entropy production rates.

Ecological applications demonstrate MEP's power and limits. Research on Siders Pond biogeochemistry showed that MEP-based models using long-term optimization (3-day intervals) produce **71% greater entropy production** (36.5 vs 21.3 GJ K^{-1}) and better match field observations than short-term (0.25-day) optimization, suggesting organisms store information in metagenomes enabling temporal strategies that maximize entropy production when averaged over time rather than instantaneously. This distinguishes biological systems from purely physical ones following steepest descent pathways. Plant optimization theories unify under MEP framework—photosynthesis optimization corresponds to maximizing entropy production associated with carbon fixation, with different objective functions (fitness measures) emerging as entropy production on different spatiotemporal scales. However, the principle requires careful specification of constraints, timescales, and which entropy production terms to include, limiting its predictive power without additional system-specific information.

Cellular automata and Turing-complete biochemical networks

Cellular automata (CA) provide powerful frameworks for modeling biogeochemical cycles by demonstrating how simple local interaction rules generate complex global patterns. Forest dynamics models employing CA include Iwasa's wave regeneration model for subalpine Abies forests showing Shimagare patterns, gap expansion models analyzing total gap area and size distributions, and competition models demonstrating how local competitive advantages produce landscape-scale vegetation mosaics. The fundamental CA principle that state transitions depend only on current cell state and neighboring cell states (typically 1-8 neighbors) enables tractable computation while capturing essential spatial dynamics. Applications extend to fire spread (Karafyllidis and Thanailakis 1997), hydrological processes through CA-Markov models examining urbanization effects on watershed runoff, and lake eutrophication dynamics with early warning signals for regime shifts.

Biochemical reaction networks demonstrate remarkable computational capabilities, with rigorous proofs of Turing completeness establishing that chemical systems can perform arbitrary computations. Fages et al. (2017) solved a longstanding open problem by proving strong (uniform) Turing completeness of chemical reaction networks over finite sets of molecular species under differential semantics—a single finite CRN can simulate a Turing machine on all inputs, not just specific input sizes. Cardelli and Zavattaro (2010) demonstrated that Turing universality derives from the interplay between molecular association and dissociation, with removal of either operation eliminating completeness. DNA computing implementations by Qian

et al. (2011) achieved efficient Turing-universal computation through DNA polymer systems, with unbounded polymers serving as registers or tapes for full computation.

Synthetic biology has systematically implemented Boolean logic gates in living cells across multiple organisms. In E. coli, the landmark Gardner toggle switch (2000) used dual repressor genes creating bistable memory activated by heat or IPTG, while the Elowitz and Leibler repressilator (2000) employed three repressors in negative feedback producing oscillations. Modern implementations achieve AND gates through two-promoter systems requiring both inputs or protein complex formation from two inputs, OR gates using either promoter to activate output, NOT gates with repressor-based systems, and NAND/NOR gates showing more digital behavior with fewer intermediate states through protein-protein interactions and DNA looping. Yeast systems demonstrate CRISPR dCas9 plus T7 polymerase implementing all basic Boolean operations responding to copper and galactose, while plant systems (2023) integrate abiotic/biotic stress signals and phytohormones through AND gates using split DNA-binding domain and transcription activation domain inputs for stress detection and yield improvement.

Metabolic pathways naturally implement logic functions through regulatory networks, though designed synthetic gates achieve more digital behavior. Design parameters affecting gate performance include dissociation constants (K_d) of regulatory proteins, inducer activation levels, promoter spacing, ribosome binding site strength, and promoter characteristic curves. Applications span cancer cell identification through multi-input AND gates detecting disease markers, metabolic pathway flux control, and microbial fuel cell activation. These demonstrations establish that biochemical networks possess full computational universality, supporting the proposition that living systems operate as sophisticated information processors subject to thermodynamic constraints including Landauer's principle on information erasure costs.

Computational requirements and algorithmic complexity of Earth system prediction

Predicting biogeochemical cycle dynamics faces fundamental computational challenges from chaos, multiscale interactions, and nonlinearity. Lyapunov exponent analysis of climate models confirms mostly positive values indicating chaotic dynamics with sensitive dependence on initial conditions—tiny measurement errors grow exponentially with doubling times of **2-3 days** for weather variables. Stanford research demonstrates predictability limits decrease by several hours per degree Celsius of warming, suggesting anthropogenic climate change paradoxically reduces our ability to predict future states even as the need intensifies. The computational complexity of integrating atmospheric general circulation models (GCMs) across appropriate spatial and temporal scales requires massive supercomputing resources.

Current operational weather prediction employs supercomputers at the petaflop scale—NOAA's 2023 WCOSS upgrade provides **29 petaflops** (29×10^{15} floating-point operations per second) across twin facilities, up from 8.4 petaflops in 2018. These systems run over 20 numerical weather prediction models including the Global Forecast System, Hurricane Analysis and Forecast System, and Global Ensemble Forecast System with typical grid resolutions of 500×640

km cells, 9-20 vertical atmospheric layers, and 30-minute time steps. Recent advances to exascale computing—Oak Ridge's Frontier supercomputer achieving **1.1 exaflops** (1.1×10^{18} operations per second)—enable climate model resolution improvements from 100 km to 3 km, allowing explicit simulation of cloud processes rather than parameterization. Applications show sharper resolution maintained for longer time periods, critical for capturing extreme events and regional impacts.

Knowledge-guided machine learning (KGML) offers transformative efficiency gains by integrating physics-based process models with deep neural networks. The KGML-ag-Carbon framework (Liu et al., Nature Communications 2024) achieves **over one million times faster computation** than traditional process-based ecosys models (1.6 days on GPU versus 5.9 years on 1000 CPUs for 21-year daily field-scale quantification across U.S. Midwest) while revealing **86% more spatial detail** in soil organic carbon changes at 250m resolution versus coarse 0.5° approaches. The framework employs Gated Recurrent Units with hierarchical structure, pre-training on 14 million synthetic data points from ecosys, then fine-tuning with county-scale yield data and eddy-covariance flux tower measurements. Knowledge-guided loss functions enforce mass balance constraints (GPP - Ra - Rh = -NEE), enabling reliable predictions with minimal training data through physics-informed priors. Performance metrics show $R^2 = 0.91$-0.96 for carbon fluxes compared to ecosys $R^2 = 0.42$-0.89, demonstrating both speed and accuracy improvements.

Neuromorphic computing inspired by biological neural networks achieves dramatic energy efficiency gains over conventional architectures. Intel's Loihi chips demonstrate **4-16× energy efficiency improvements** for large neural networks through event-driven spiking neurons, integrated memory-computation, and asynchronous processing that minimizes data movement and activity. The BrainScaleS 2 system operates at 57 mW while accelerating **1000× faster than biological real-time**, with on-chip learning converging in seconds equivalent to hours biologically. Two-dimensional transition metal dichalcogenide (2D-TMD) tunnel-FET neuromorphic circuits achieve **two orders of magnitude higher energy efficiency** than silicon-based 7nm FinFET technology through leaky-integrate-fire neurons with Hebbian learning. These bio-inspired approaches exploit population dynamics enabling the human brain's **100 billion neurons** to consume merely **20 watts**—equivalent to an energy-saving light bulb—by processing primarily meaningful changes (events) rather than continuous signals, storing information locally to avoid von Neumann bottlenecks, and optimizing network-level energy rather than individual component efficiency.

Scaling laws from metabolic theory to hydrological fractals

Universal scaling relationships govern biological and physical systems across enormous size ranges, revealing deep constraints from network architecture and thermodynamic optimization. Metabolic scaling theory developed by West, Brown, and Enquist establishes that basal metabolic rate scales as the **3/4 power of body mass**: **$B \propto M^{(3/4)}$** across 27 orders of magnitude from cytochrome oxidase molecules to blue whales. This quarter-power scaling emerges from three principles governing hierarchical branching resource distribution networks: (1) space-filling networks reaching all tissues; (2) size-invariant terminal units like capillaries; and (3) minimization of energy and time to distribute resources. Additional quarter-power

exponents follow—cellular metabolic rates scale as M^(-1/4), heart and respiratory rates as M^(-1/4), circulation times and lifespans as M^(1/4), and remarkably, numbers of leaves (petioles) in plants scale as M^(3/4), suggesting universal principles extend beyond animal physiology to plant architecture.

The fractal network foundation explains these exponents through space-filling branching geometries. Each bifurcation optimally balances two competing constraints: maintaining sufficient flow to supply all tissues while minimizing energy dissipation in transport. The resulting fractal dimension and branching ratios produce 3/4 power scaling when networks span from molecular pumps (capillaries, stomata) through hierarchical branches to organism-scale distribution. Some researchers argue for 2/3 power scaling based on surface area to volume ratios for heat dissipation, with empirical measurements reporting values between 2/3 and 3/4 depending on taxa and conditions, but the weight of evidence and theoretical foundation supports the 3/4 exponent as fundamental under resource distribution constraints. The theory quantitatively predicts not just metabolic rate but forest structure dynamics, population growth rates, mutation rates, and population densities as functions of organism size.

Hydrological systems exhibit analogous fractal organization. Rodríguez-Iturbe and Rinaldo's seminal work "Fractal River Basins: Chance and Self-Organization" (1997) established that river networks show scaling and multi-scaling properties with self-similar and self-affine characteristics arising from self-organized criticality during network development. Branching networks arrange following minimum energy expenditure principles, producing power law relationships between discharge, drainage area, and slope with specific fractal dimensions characterizing drainage density, stream length, and topology. The Geomorphologic Instantaneous Unit Hydrograph links unit hydrograph response to geomorphologic parameters, providing theoretical basis for basin arrangement applicable across variations in size, climate, and geology. These fractal principles enable prediction of hydrological responses from topographic structure and explain universal features of drainage networks worldwide.

Ecosystem organization reflects similar optimization principles. Maximum entropy production in living systems may drive evolution of fractal-like biomass distribution networks (roots, mycorrhizal networks, vascular systems) that maximize energy dissipation and nutrient cycling rates given spatial and material constraints. Forest vertical structure shows power law scaling of biomass with height, gap size distributions follow power laws, and species abundance patterns often fit log-series or power law distributions. These scaling relationships suggest ecosystems organize to utilize available energy gradients efficiently through hierarchical networks, with quarter-power or similar exponents emerging from geometric and thermodynamic optimization. The convergence of scaling laws across metabolic physiology, hydrological geomorphology, and ecological structure points to universal principles governing how networks organize to move materials, energy, and information through hierarchical branching architectures under thermodynamic constraints.

Quantum mechanics to ecosystems: statistical mechanics foundations and emergent irreversibility

The connection from quantum mechanics to ecosystem-scale patterns proceeds through statistical mechanics and entropy. Quantum systems evolve according to the time-reversible Schrödinger equation, with unitary evolution preserving information and microstate probabilities. Yet macroscopic systems exhibit clear irreversibility and entropy increase. The resolution emerges through the Boltzmann entropy formula **$S = k_B \ln(\Omega)$** relating macroscopic entropy to the number of accessible microstates Ω. For quantum systems, Ω counts quantum states; for classical systems, phase space divides into cells of size h^(3N) where h is Planck's constant and N is particle number. The second law stating entropy increases ($dS/dt \geq 0$ for isolated systems) follows statistically—systems evolve toward macrostates with larger Ω because high-entropy states are overwhelmingly more numerous than low-entropy states. Microscopic time-reversibility coexists with macroscopic irreversibility through statistical averaging over vast particle numbers, with spontaneous entropy decrease probability scaling as $\exp(-\Delta S/k_B) \sim \exp(-10^{23})$ for macroscopic systems.

Quantum coherence in photosynthetic light harvesting generated excitement when 2007 experiments by Engel et al. detected quantum beating signals lasting ~600 femtoseconds at 77K in the Fenna-Matthews-Olson complex, suggesting wavelike energy transfer exploring multiple pathways simultaneously might enhance efficiency. However, subsequent research demonstrated that at physiological temperatures (300K), electronic coherence decays in under 60 femtoseconds—likely too brief for functional significance. Comprehensive studies (Cao et al. 2020, Duan et al. 2017) in Science Advances and PNAS concluded quantum coherence does not substantially enhance photosynthetic efficiency, with observed oscillations primarily representing vibrational rather than electronic coherence. Classical incoherent hopping suffices to explain photosynthesis's ~100% quantum yield. While some quantum effects persist (tunneling, excitonic delocalization, vibrational zero-point energy), coherent superposition probably plays minimal functional role. The scaling from quantum molecular processes to ecosystem carbon fixation proceeds primarily through classical thermodynamics—photosynthetic efficiency determines light-use efficiency, affecting growth rates, competitive fitness, and primary productivity, with the 500 Gt C/year globally fixed representing energy capture limited by thermodynamic efficiencies rather than quantum coherence effects.

Maximum entropy production versus minimum entropy production principles operate in different regimes. Prigogine's theorem (1947) states that in the steady state of linear non-equilibrium systems near thermodynamic equilibrium, entropy production reaches its minimum value under constant external constraints. This applies when flux-force relationships are linear (Onsager relations valid), providing a Lyapunov function proving system stability. However, validity requires very close approach to equilibrium—for chemical reactions, only near chemical equilibrium. Far from equilibrium where biogeochemical cycles operate, linearity breaks down and minimum entropy production no longer applies. MEP principle conversely applies to far-from-equilibrium systems, proposing they adapt to states maximizing entropy production. These principles do not contradict—Prigogine describes transient evolution toward steady states near equilibrium; MEP describes selection among possible steady states far from equilibrium. Most living systems operate far from equilibrium, making MEP potentially relevant while Prigogine's theorem applies only to limited near-equilibrium subsystems.

Self-organization in dissipative structures provides the mechanistic link from thermodynamic gradients to ecosystem patterns. Prigogine's Nobel Prize work established that thermodynamically open systems far from equilibrium spontaneously form ordered patterns through energy dissipation—classic examples include Bénard convection cells forming hexagonal patterns when fluid is heated from below above critical Rayleigh number, and Belousov-Zhabotinsky reactions producing spiral waves through autocatalytic chemistry. Living cells represent dissipative structures maintaining organization far from equilibrium through continuous energy and material flows. The mechanism proceeds: (1) thermodynamic gradient imposed on system; (2) instability develops when gradient exceeds threshold; (3) autocatalytic feedback amplifies fluctuations; (4) organized structure emerges efficiently dissipating gradient; (5) higher entropy production in organized versus disordered state. Ecosystem succession may follow this pattern—bare ground develops vegetation increasing evapotranspiration, deepening roots, lowering albedo, all enhancing energy capture and entropy production. Forest development studies confirm entropy production increases during succession, supporting the view that ecosystems self-organize to accelerate gradient dissipation, consistent with MEP principles though not proving them uniquely correct.

Environmental AI design principles: from maximum entropy to knowledge-guided learning

Information-theoretic optimization principles enable substantial improvements in environmental monitoring network design, sensor placement, and observational strategies. Entropy-based approaches select sensor locations maximizing joint information (Shannon entropy) while minimizing redundancy (mutual information between sensors), achieving high representativeness with minimal sensor count. Urban drainage system studies demonstrate that optimally placed sensor networks achieve **76% flooding risk assessment accuracy** with merely 4 sensors and **33% operation status perception error** through information maximization. Environmental sensor network design employs evolutionary algorithms finding optimal placements in regions of interest, with spatial regression tests ensuring networks maintain performance when sensors fail. The fundamental principle treats sensors as information sources with informativity quantified by Shannon entropy accounting for pollution dispersion, meteorology, and topography—placing sensors where they reduce uncertainty most effectively per unit cost.

Knowledge-guided machine learning represents a paradigm shift for biogeochemical cycle monitoring by encoding physical laws directly into neural network architectures and loss functions. The KGML-ag-Carbon framework demonstrates the power of this approach: pre-training deep learning models on millions of synthetic data points from process-based ecosys simulations provides physics-informed priors, then fine-tuning on limited real observations (as few as 2-10 counties versus 320 required for pure ML) achieves superior performance. The knowledge-guided loss function enforces carbon mass balance **GPP - Ra - Rh = -NEE**, preventing physically impossible predictions. This integration enables the model to interpolate and extrapolate reliably despite sparse training data, achieving 250m spatial resolution predictions across entire regions—resolution where field-level carbon management decisions occur. The approach generalizes: encoding conservation laws (mass, energy, momentum),

thermodynamic constraints (entropy increase, Gibbs free energy), or scaling relationships directly into neural networks enables learning from limited data while respecting physical reality.

Optimal control of ecosystems through MEP principles offers a quantitative framework for nature-based solutions design. The 2010 Royal Society theme issue established that plant optimization theories unify under MEP—photosynthesis optimization corresponds to maximizing entropy production associated with carbon fixation, with different fitness measures emerging as entropy production on different spatiotemporal scales. Living systems store information in metagenomes enabling temporal optimization strategies, maximizing entropy production when averaged over ecologically relevant timescales (3-day intervals for pond ecosystems produced 71% higher entropy production than 0.25-day myopic optimization). This suggests ecosystem management should consider how systems naturally organize to dissipate gradients efficiently, designing interventions that enhance rather than impede these tendencies. Restoration efforts might focus on removing bottlenecks to energy and nutrient flows, establishing hierarchical network structures following fractal optimization principles, and maintaining biodiversity that enables complete gradient utilization across varying conditions.

Neuromorphic computing offers AI energy efficiency improvements of 4-16× for environmental applications by mimicking biological neural network architectures. Event-driven information encoding transmits and processes only meaningful changes, minimizing operations. Computing-in-memory architectures like brain synapses eliminate von Neumann bottlenecks from shuttling data between separate processors and memory. Spike-timing-dependent plasticity enables on-chip learning. Applications to environmental monitoring include autonomous vehicle sensor processing, satellite systems, predictive maintenance, and edge AI where energy efficiency and low latency prove critical. The human brain's ability to process 100 billion neurons on 20 watts through population-level energy optimization rather than component optimization provides the design paradigm—Growth Transform Neural Networks frame neuromorphic systems as network-level energy optimization problems, using fewer spikes than traditional architectures while encompassing all neurons with easier training potential. Scaling to billions of neurons without explicit spike routing becomes feasible, offering paths toward environmental AI systems that process planetary-scale data streams with biological energy efficiency.

Emerging synthesis and future directions

The convergence of information theory, thermodynamics, and biogeochemical science reveals Earth's living systems as sophisticated computational engines processing energy and information under universal physical constraints. Several fundamental principles emerge as candidates for guiding environmental superintelligence. First, **maximum entropy production when averaged over appropriate temporal scales** appears to govern ecosystem organization far from equilibrium, with living communities augmenting entropy production 1,000-10,000-fold over abiotic alternatives through information storage in genetic code enabling temporal optimization strategies exceeding greedy myopic approaches. Second, **universal scaling laws following quarter-power exponents** across 27 orders of magnitude from fractal hierarchical network architectures suggest optimal resource distribution fundamentally constrains biological and physical organization. Third, **the equivalence of Shannon information entropy and Boltzmann thermodynamic entropy** established by Jaynes provides rigorous foundation for

treating information as physical quantity subject to thermodynamic laws, with Landauer's principle setting fundamental computational efficiency limits at $k_B T \ln(2)$ per bit erased.

Fourth, **biological systems approach thermodynamic efficiency limits** remarkably closely—protein translation operates 26× above Landauer bounds, approximately one million times more efficiently than current supercomputers, suggesting billions of years of natural selection optimized molecular machinery. Fifth, **knowledge-guided machine learning** integrating physical laws achieves million-fold computational speedups over process-based models while requiring minimal training data, demonstrating power of combining symbolic knowledge with statistical learning. Sixth, **fundamental predictability limits** from chaos theory and positive feedbacks constrain uncertainty reduction regardless of observational or computational improvements, requiring ensemble methods and conformal inference for rigorous uncertainty quantification. Seventh, **self-organization in dissipative structures** far from equilibrium demonstrates how thermodynamic gradients drive pattern formation through instabilities, autocatalysis, and symmetry breaking, with organized states exhibiting higher entropy production than disordered alternatives.

These principles suggest design heuristics for environmental AI: optimize network-level energy efficiency through event-driven computation and computing-in-memory architectures rather than component optimization; exploit hierarchical fractal structures for information and resource distribution; maximize information gain per unit entropy produced through optimal sensor placement using information theory; encode physical constraints directly into learning algorithms as knowledge-guided priors; employ temporal strategies that optimize over ecologically relevant timescales rather than instantaneous optimization; and recognize fundamental predictability limits requiring probabilistic approaches with rigorous uncertainty quantification rather than deterministic prediction.

Research priorities include bridging scales from molecular to planetary, integrating multiple biogeochemical cycles (C-N-P-S interactions), characterizing deep uncertainties that resist probabilistic quantification, and developing portable knowledge modules enabling transfer learning across ecosystems and regions. Hardware innovation in neuromorphic computing promises 100× energy efficiency gains through 2D transition metal dichalcogenide tunnel-FET devices and 3D stacked synapse fabrics. Theoretical work should clarify conditions under which MEP applies versus fails, derive MEP rigorously from first principles if possible, and elucidate connections between quantum effects in biological systems and macroscopic ecosystem properties through statistical mechanics.

The vision of environmental superintelligence emerges as systems that process planetary-scale data streams with biological efficiency through neuromorphic architectures, learn from limited observations by integrating physical laws as knowledge priors, predict within fundamental limits using ensemble and information-theoretic methods, and guide management toward configurations that enhance natural entropy production tendencies through removal of bottlenecks and establishment of optimized network structures. The deep truth underlying this vision may be that life exists because it accelerates entropy production over greater spatiotemporal scales than abiotic processes—not through violation of physical laws but through information storage enabling temporal strategies, hierarchical network architectures minimizing

energy per transported resource, and self-organization that efficiently dissipates thermodynamic gradients. An environmental AI aligned with these principles would not fight nature but amplify its fundamental tendencies, becoming a partner in Earth's computational-thermodynamic processing of solar energy gradients into increasing entropy while maintaining transient low-entropy organization that we experience as the living biosphere.